Molecular Crystals and Liquid Crystals

Publication details, including instructions for authors and subscription information:
http://www.tandfonline.com/loi/gmcl20

Synthesis and Characterization of Banana-Shaped Mesogens Derived From a Benzophenone Moiety

K. C. Majumdar [a], Santanu Chakravorty [a], Randhir Kumar Sinha [a] & Nilasish Pal [a]

[a] Department of Chemistry, University of Kalyani, Kalyani, West Bengal, India

Version of record first published: 17 Dec 2009

To cite this article: K. C. Majumdar, Santanu Chakravorty, Randhir Kumar Sinha & Nilasish Pal (2009): Synthesis and Characterization of Banana-Shaped Mesogens Derived From a Benzophenone Moiety, Molecular Crystals and Liquid Crystals, 515:1, 125-134

To link to this article: http://dx.doi.org/10.1080/15421400903291392

Mol. Cryst. Liq. Cryst., Vol. 515, pp. 125–134, 2009

ISSN: 1542-1406 print/1563-5287 online
DOI: 10.1080/15421400903291392

Taylor & Francis
Taylor & Francis Group

Synthesis and Characterization of Banana-Shaped Mesogens Derived From a Benzophenone Moiety

K. C. Majumdar, Santanu Chakravorty, Randhir Kumar Sinha, and Nilasish Pal
Department of Chemistry, University of Kalyani, Kalyani, West Bengal, India

A homologous series of Schiff's bases consisting of a benzophenone moiety as the central core has been synthesized. Schiff's bases were prepared starting from benzophenone by a sequence of reactions, viz., nitration followed by reduction and heating the resulting diamino derivative with 4-formyl-3-hydroxyphenyl 4-(alkyloxy)benzoate. Higher homologues of this series exhibit mesomorphism, but the lower homologues do not seem to possess any liquid crystalline property. The B_2 mesophase was characterized by DFT study for orientation of dipole moment. Dipolar interaction and intramolecular H-bonding (N–H) have been considered to discuss the origin of the B_2 phase in this homologous series of benzophenone moiety derived systems.

Keywords: B_2 phase; bent shape; DFT; DSC; POM; Schiff's base

INTRODUCTION

Conventional thermotropic liquid crystals are formed by anisometric molecules (mesogens that are either rod shaped or disc shaped). Nematic or smectic phases are preferred by rod-like molecules ("calamatic compounds") [1], and the smectic phase possesses one dimensional density modulation. Disc-like molecules (discotic compounds) [2–4] can also show the nematic phase, but they generally prefer to form columnar phases with a two-dimensional modulated structure. If the shape of the molecule significantly deviates from the classical rod- or disc-like shape, new phases as well as subphases of well-known phases occur [5–9]. An interesting example is bent core

Address correspondence to K. C. Majumdar, Department of Chemistry, University of Kalyani, Kalyani 741235, West Bengal, India. E-mail: kcm_ku@yahoo.co.in

mesogens, which are the subject of extensive investigations during the last few years in particular because of their new mesophases with unusual properties compared to smectic phases formed by calamatic compounds. Vorlander and Apel [10,11] first reported this type of bent-core molecules. This type of molecule can be broadly classified into two categories: a) V-shaped and b) banana-shaped. Disubstitution at the 1,2- or 1,3-position of the benzene ring can generate bent-shaped molecules. Specifically 1,2-disubstitution generates V-shaped molecules [12] and disubstitution at 1,3-position results in banana-shaped [13–15] molecules. Very recently we too have reported the liquid crystalline properties of such bent-shaped molecules with a furan-bridge at the core [16]. B-phases are found in five-, six-, and seven-ring systems having an angle between the two molecular axes from more than 130° to less than 100°. In this article, we present a new class of bent-shaped molecules in which central core is different from that reported by others, and the molecules contain six aromatic rings. As a part of our ongoing effort to realize new materials [17–22] to explore the limits of molecular shapes compatible with liquid crystalline behavior, and to study the structure property relationship, we have undertaken a study on the synthesis and characterization of bent mesogens based on 3,3-disubstituted benzophenone rather than 1,2-disubstituted benzene, in the core with Schiff's base linkage. Here we report the results.

2. EXPERIMENTAL

The methodology of synthesis of the banana-shaped materials **6a–e** is depicted in Scheme 1. Benzophenone was first converted into its dinitro derivative (**2**), which was then reduced to the diamine derivative (**3**). The diamino derivative **3** was then heated under reflux with 4-formyl-3-hydroxyphenyl 4-(alkyloxy)benzoates in absolute ethanol in the presence of a catalytic amount of glacial acetic acid to afford the homologous series **6a–e**. The compounds **6a–e** were characterized from their elemental analyses, ^{1}H NMR and IR spectra.

All the chemicals were procured from either Sigma Aldrich Chemicals Pvt. Ltd. or Spectrochem, India. Silica gel [(60–120 mesh) was used for chromatographic separation. Silica gel G [E-Merck (India)] was used for TLC. Petroleum ether refers to the fraction boiling between 60°C and 80°C. IR spectra were recorded on a Perkin-Elmer L 120–000A spectrometer (ν_{max} in cm^{-1}) on KBr disks. UV absorption spectra were recorded in $CHCl_3$ on a Shimadzu UV-2401PC spectrophotometer (λ_{max} in nm). ^{1}H NMR (300 MHz) spectra were recorded on a Bruker DPX-500 spectrometer in $CDCl_3$ (chemical shift in δ) with

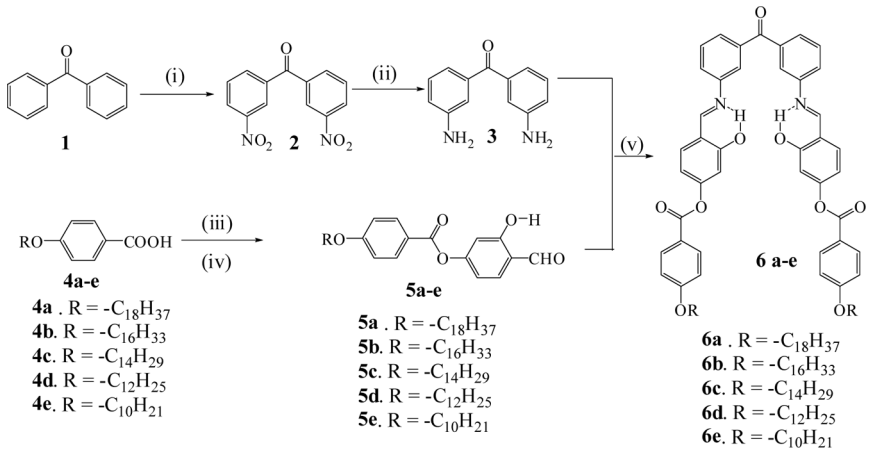

SCHEME 1 Reaction conditions and reagents: (i) fuming HNO_3/Conc. H_2SO_4 (1:4, 10 ml/g), heat, 60°C, 2 h (ii) ethyl acetate, $SnCl_2 \cdot 2H_2O$, conc. HCI (cat), reflux, 4 h; (iii) $SOCL_2$, reflux, 1 h; (iv) 2,4-dihydroxy benzaldehyde, DCM, aq K_2CO_3, Bu_4NHSO_4, 12 h; (v) dry EtOH, glacial AcOH, reflux, 4 h.

TMS as internal standard. CHN was recorded on 2400 series II CHN analyzer Perkin Elmer. The liquid crystalline properties were established by thermal microscopy (Nikon polarizing microscope LV100POL attached to an Instec hot and cold stage HCS302, with STC200 temperature controller configured for HCS302 and the phase transitions were confirmed by differential scanning calorimetry (Perkin-Elmer Diamond DSC system).

2.1.

3,3′-Dinitrobenzophenone **2** and 3,3′-diaminobenzophenone **3** were prepared according to the published procedure [23].

2.2. General Procedure for the Preparation of Compounds 6a–e

3,3′-Diaminobenzophenone **3** (0.05 g, 0.02 mmol) was heated under reflux with 4-formyl-3-hydroxyphenyl 4-(octyloxy)benzoate **5a** (0.025 g, 0.048 mmol) in absolute ethanol in the presence of a catalytic amount of glacial acetic acid to afford the desired product **6a**. All the other compounds were prepared according to the same procedure.

Compound: 6a

Yield 86%, Pale yellow solid; IR (KBr) ν_{max}: 2915, 2850, 1725, 1651, 1611 cm^{-1}; ^{1}H-NMR ($CDCl_3$, 400 MHz): δ_H 13.29 (s, 2 H), 8.69 (s, 2 H), 8.14 (d, $J = 8.8$ Hz, 4 H), 7.70–7.73 (m, 4 H), 7.52–7.59 (m, 4 H), 7.44 (d, $J = 8.4$ Hz, 2 H), 6.95 (d, $J = 8.8$ Hz, 4 H), 6.89 (d, $J = 1.7$ Hz, 2 H), 6.86 (dd, $J = 8.3$, 2.3 Hz, 2 H), 4.02 (t, $J = 6.5$ Hz, 4 H), 1.79–1.83 (quin, 4 H, $J = 7.6$ Hz), 1.24–1.54 (m, 60 H), 0.85 (t, $J = 6.9$ Hz, 6 H); ^{13}C-NMR ($CDCl_3$, 100 MHz): 195.49, 164.31, 163.72, 163.09, 162.59, 155.26, 148.74, 138.64, 133.50, 132.39, 129.55, 128.45, 125.83, 122.02, 121.12, 116.90, 114.36, 113.37, 110.72, 68.40, 31.92, 29.69, 29.58, 29.56, 29.36, 29.07, 25.97, 22.69, 14.11; Anal Calcd. For $C_{77}H_{100}N_2O_9$, C, 77.22; H, 8.42; N, 2.34; Found, C, 77.38, H, 8.52, N, 2.40%.

Compound: 6b

Yield 90%, Pale yellow solid; IR (KBr) ν_{max}: 2916, 2850, 1726, 1652, 1610 cm^{-1}; δ_H 13.30 (s, 2 H), 8.72 (s, 2 H), 8.10 (d, $J = 8.6$ Hz, 4 H), 7.72–7.76 (m, 4 H), 7.50–7.56 (m, 4 H), 7.47 (d, $J = 8.3$ Hz, 2 H), 6.94 (d, $J = 8.6$ Hz, 4 H), 6.92 (d, $J = 2.0$ Hz, 2 H), 6.82 (dd, $J = 8.3$, 2.0 Hz, 2 H), 4.01 (t, $J = 6.4$ Hz, 4 H), 1.77–1.84 (quin, 4 H, $J = 6.5$ Hz), 1.24–1.46 (m, 52 H), 0.85 (t, $J = 6.9$ Hz, 6 H); ^{13}C-NMR ($CDCl_3$, 100 MHz): 195.48, 164.24, 163.70, 163.05, 162.56, 155.25, 148.71, 138.64, 133.47, 132.35, 129.50, 128.38, 125.78, 122.00, 121.10, 116.87, 114.34, 113.33, 110.68, 68.34, 31.90, 29.67, 29.63, 29.56, 29.53, 29.33, 29.06, 25.95, 22.66, 14.09; Anal Calcd. For $C_{73}H_{92}N_2O_9$: C, 76.81; H, 8.12; N, 2.45; Found, C, 76.93, H, 8.20, N, 2.52.

Compound: 6c

Yield 90%, Pale yellow solid; IR (KBr) ν_{max}: 2916, 2850, 1726, 1652, 1610 cm^{-1}; ^{1}H-NMR ($CDCl_3$, 400 MHz): δ_H 13.32 (s, 2 H), 8.72 (s, 2 H), 8.14 (d, $J = 8.8$ Hz, 4 H), 7.74–7.77 (m, 4 H), 7.57–7.60 (m, 4 H), 7.47 (d, $J = 8.3$ Hz, 2 H), 6.98 (d, $J = 8.8$ Hz, 4 H), 6.92 (d, $J = 2.3$ Hz, 2 H), 6.86 (dd, $J = 8.3$, 2.3 Hz, 2H), 4.05 (t, $J = 6.6$ Hz, 4 H), 1.81–1.88 (quin, 4 H, $J = 6.3$ Hz), 1.28–1.58 (m, 44 H), 0.88 (t, $J = 7.0$ Hz, 6 H); ^{13}C-NMR ($CDCl_3$, 100 MHz): 195.5, 164.30, 163.74, 163.09, 162.59, 155.29, 148.74, 138.67, 133.51, 132.39, 129.55, 128.43, 125.83, 122.04, 121.12, 116.90, 114.37, 113.38, 110.72, 68.37, 31.93, 29.67, 29.60, 29.57, 29.37, 29.10, 25.98, 22.70, 14.13; Anal Calcd. For: $C_{69}H_{84}N_2O_9$, C, 76.35; H, 7.80; N, 2.58; Found, C, 76.55, H, 7.92, N, 2.67.

Compound: 6d

Yield 90%, Pale yellow solid; IR (KBr) ν_{max}: 2915, 2850, 1726, 1651, 1610 cm^{-1}; ^{1}H-NMR ($CDCl_3$, 400 MHz): δ_H 13.32 (s, 2 H), 8.72 (s, 2 H), 8.14 (d, $J = 9.0$ Hz, 4 H), 7.74–7.77 (m, 4 H), 7.57–7.60 (m, 4 H), 7.47

(d, $J = 8.6$ Hz, 2 H), 6.98 (d, $J = 9.0$ Hz, 4 H), 6.92 (d, $J = 2.0$ Hz, 2 H), 6.86 (dd, $J = 8.6$, 2.0 Hz, 2 H), 4.05 (t, $J = 6.6$ Hz, 4H), 1.82–1.86 (quin, 4 H, $J = 7.8$ Hz), 1.29–1.57 (m, 36 H), 0.88 (t, $J = 7.0$ Hz, 6 H); ^{13}C-NMR ($CDCl_3$, 100 MHz): 195.56, 164.32, 163.79, 163.13, 162.65, 155.34, 148.77, 138.72, 133.57, 132.44, 129.60, 128.47, 125.86, 122.10, 121.18, 116.96, 114.43, 113.41, 110.76, 68.43, 31.98, 29.72, 29.70, 29.65, 29.62, 29.42, 29.15, 26.04, 22.75, 14.18; Anal Calcd. For: $C_{65}H_{76}N_2O_9$, C, 75.85; H, 7.44; N, 2.72; Found, C, 75.99, H, 7.53, N, 2.76.

Compound: 6e

Yield 90%, Pale yellow solid; IR (KBr) ν_{max}: 2915, 2850, 1725, 1651, 1610 cm^{-1}; ^{1}H-NMR ($CDCl_3$, 400 MHz): δ_H 13.32 (s, 2 H), 8.72 (s, 2 H), 8.14 (d, $J = 8.8$ Hz, 4 H), 7.73–7.76 (m, 4 H), 7.55–7.62 (m, 4 H), 7.47 (d, $J = 8.5$ Hz, 2 H), 6.98 (d, $J = 8.8$ Hz, 4 H), 6.92 (d, $J = 2.0$ Hz, 2 H), 6.86 (dd, $J = 8.5$, 2.0 Hz, 2 H), 4.05 (t, $J = 6.6$ Hz, 4 H), 1.82–1.86 (quin, 4 H, $J = 8.0$ Hz), 1.51–1.86 (m, 28 H), 0.89 (t, $J = 7.0$ Hz, 6 H); ^{13}C-NMR ($CDCl_3$, 100 MHz): 195.55, 164.30, 163.74, 163.09, 162.59, 155.28, 148.72, 138.66, 133.52, 132.40, 129.55, 128.44, 125.83, 122.05, 121.12, 116.91, 114.38, 113.38, 110.72, 68.37, 31.90, 29.56, 29.37, 29.32, 29.09, 25.98, 22.69, 14.13; Anal Calcd. For: $C_{61}H_{68}N_2O_9$, C, 75.28; H, 7.04; N, 2.88; Found, C, 75.37, H, 7.15, N, 2.97.

3. RESULTS AND DISCUSSION

The transition temperatures and associated enthalpies of all the compounds of the series were determined by differential scanning calorimetry (DSC) and are represented in Table 1. In the DSC scan we observed several solid–solid transitions (and/or crystalline smectic–smectic) transitions for **6a** and **6b** with small but noticeable enthalpy changes (<3.7 KJ/mole), which were not observed by thermal microscopy and by DSC scan on the cooling cycle. We observed no such transition for lower homologues of the series.

The solid–liquid crystal phase transition recorded in the heating cycle is confirmed by thermal microscopy. DSC scans of higher homologues of the series (**6a, 6b, 6c**) showed only one liquid crystalline phase transition, but the lower homologues (**6d, 6e**) of the series with a short alkoxy chain at the terminal position exhibited no mesophase behavior. The enthalpy recorded at the liquid crystalline phase-isotropic transition is much higher than that of the solid–liquid crystalline phase transition, which is not uncommon in bent shaped molecules. The difference in enthalpy value from the first and subsequent heating/cooling cycles is probably due to the ordered arrangement of molecules within each layer which must have been driven by minimized steric packing

TABLE 1 Phase Transition Temperature (°C) and Associated Enthalpies (ΔH, KJmole^{-1}) of Compounds **6a–e**

6a:

$$Cr_1 \xrightarrow[2.9]{114.68} Cr_2 \xrightarrow[26.0]{130.71} B2 \xrightarrow[53.2]{155.26} I \xrightarrow[33.9]{149.40} B2 \xrightarrow[16.4]{142.5} Cr$$

6b:

$$Cr_1 \xrightarrow[0.1]{126.58} Cr_2 \xrightarrow[3.6]{129.33} Cr_3 \xrightarrow[10.6]{133.92} B2 \xrightarrow[47.4]{155.37} I \xrightarrow[23.3]{149.02} B2 \xrightarrow[11.0]{145.52} Cr$$

6c:

$$Cr \xrightarrow[10.2]{133.31} B2 \xrightarrow[47.6]{156.67} I \xrightarrow[28.8]{149.54} B2 \xrightarrow[18.9]{147.28} Cr$$

6d:

$$Cr \xrightarrow[42.0]{162.05} I \xrightarrow[39.1]{152.82} Cr$$

6e:

$$Cr \xrightarrow[43.0]{163.75} I \xrightarrow[40.1]{154.21} Cr$$

forces as well as minimization of coulombic free energy to an ordered arrangement of the molecules that sets in during the solidification process. The enthalpy change that occurred during the phase transition is sufficiently larger for compounds **6a–e**. This may be due to the presence of intramolecular H-bonding (which is confirmed by the presence of a one proton singlet at $\delta_H \sim 13.3$ ppm in the ^{1}H NMR of compounds **6a–e**). The observed optical texture of compound **6c** is represented in Fig. 1a,b. The phase generated on heating could not be identified. However, a fan-like texture gradually appeared from the isotropic phase

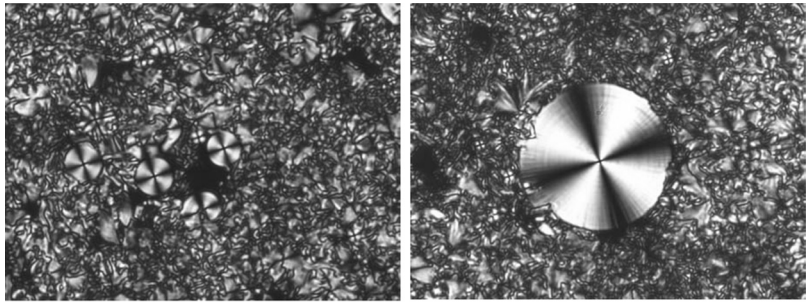

(a) (b)

FIGURE 1 (a) Fan like texture of **6c** at 148°C at 20X. (b) Fan like texture of **6c** at 148.2°C at 50X.

on slow cooling and strongly developed at 148°C clearly indicating the existence of a B_2 phase, a characteristic of bent-shaped molecules. Compounds **6a** and **6b** also showed similar phase behavior on POM study. However, the other two lower homologues **(6d, 6e)** did not show any liquid crystalline phase transition. In most cases, the angle between the molecular long axes is about 120°. When the bending angle is lower than 100°, nematic and smectic phases also appear in addition to the B_2 phase [24].

Dipolar interaction plays an important role in stabilizing the liquid crystalline phases. B_2 is a tilted smectic phase having monolayer structure with polar order. The textural appearance with the molecular structure having a long terminal chain (C_{14}, C_{16}, C_{18}) suggested that the phase should be B_2 type rather than B_1 or B_6. It is a well-known fact that if the terminal chain length is short, e.g., C_6 the nematic (N) and intercalated smectic phase (B_6) is often observed. The elongation of chains disfavors the formation of B_1 and polar smetic phases with monolayer structure (B_2). Hence phase sequence B_6-B_1-B_2 is often observed with increasing chain length [25,26]. The direction of the dipole of the compound **6c** was calculated by Density Functional Theory (DFT), which may determine the presence of dipolar interaction within the molecules. All calculations have been performed by the Chem3D (version 10) [27] with GAUSSIAN 03 Interface [28]. We have computed the DFT (B3LYP) level of theory using the basis set 6–31 G to obtain the dipole moment and dipolar orientation of molecules. The dipole moment of **6c** have been calculated as 13.7706 D ($X = 9.0864$, $Y = -8.3206$, $Z = 6.1509$). After geometry optimization of the compound **6c** (Fig. 2) by addition of atoms step by step, the optimized structure suggests that the molecule possess a V shape.

The first optimization was done by the MM2 method followed by the AM1 method, and finally DFT was performed as stated earlier. The high dipole moment (13.7706 D) of **6c** indicates the presence of H-bonding (N–H) as also evident from IR and ^{1}H NMR. If we suppose Z-axis as molecular axis and the maxima of dipole moment is in the positive X-axis direction (9.0864 D), the direction of net dipole moment should be transverse to molecular axis. Near-neighbour antiparallel correlation of molecules within the layer of B_2 phase will occur in reality if the direction of dipole is transverse/longitudinal. The bent direction in adjacent layers should be antiparallel, so that the layer polarization alternates from layer to layer; leading to a macroscopic apolar antiferroelectric structure which is applicable to B_2 with switching behavior. Within the layers the molecules are in most cases additionally tilted parallel to the polar direction in the case of the $SmCP_A$ or B_2 phases. However, there are a few reports where non-tilted $SmAP_A$

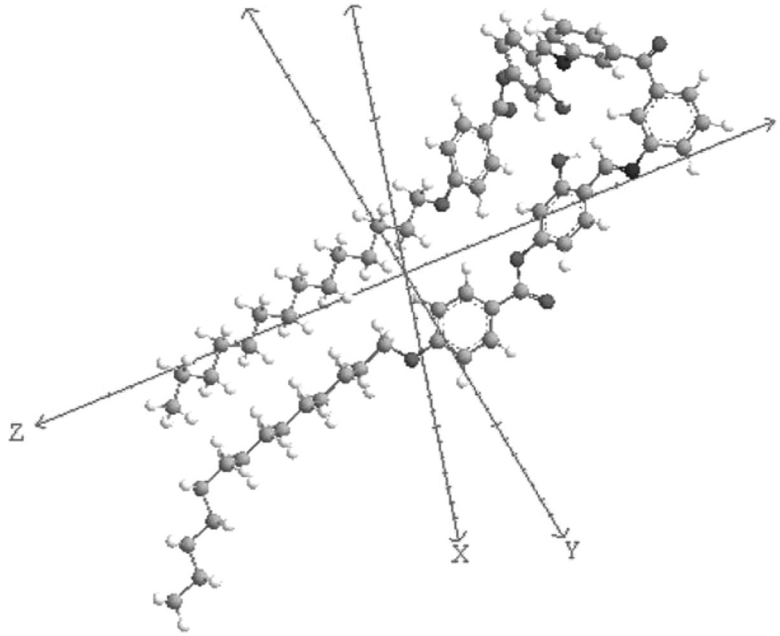

FIGURE 2 Optimized geometry of compound **6c** by DFT (B3LYP) level of theory using the basis set 6-31G.

structures were also observed [29]. DFT study suggests that the near-neighbour antiparallel correlation exists and in broad-on side position with respect to the direction of dipole within the layers. Based on the direction of the dipole moment, calculated from DFT and considering the presence of H-bonding we have constructed a model of supramolecular arrangement in B_2 phase which is depicted in Fig. 3.

Textural appearance of **6c** and DFT study for geometry optimization suggest that the compound **6c** possesses a B_2 phase rather than any other banana mesophase as the molecule is bent shaped. In general, the achiral banana-shaped molecular systems that generate reduced symmetry mesophases normally consist of five aromatic rings. In our present study, the compounds **6a–e** possess six-ring structures. Additionally, in the present instance, we have used 3,3′-disubstituted benzophenone as a core with Schiff's base linkage. It is relevant to mention that Schiff base linkage is well known in standard calamatic system [30–33]. This is because they are resistance to thermal and hydrolytic degradation. Most importantly, they can be substituted with different entities and readily coordinate with a range of metal ions to

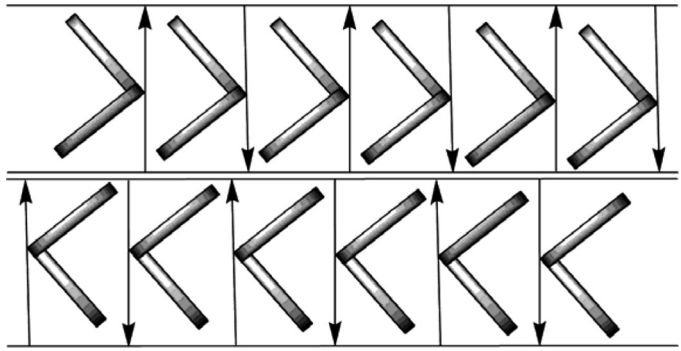

FIGURE 3 Molecular organization within the polar smectic phase SmCP or B_2 base direction of dipole moment derived from DFT. The arrows indicate the direction of the dipole moment.

form metallomesogens. There are also several examples of the introduction of hydroxyl group (Schiff base linkage) in one of the arms of banana-shaped material to stabilize the phase [22,34]. However, in this particular case, we have used Schiff's base linkage to stabilize the existing liquid crystalline phase and to maintain proper geometry of the banana-shaped material. To the best of our knowledge, there is no report of 3,3′-disubstituted benzophenone containing V-shaped liquid crystal. We are continuing this work with the new class of organic mesogens, and a full account will be communicated later. The demonstration of antiferroelectricity could be the theme of future exploration.

ACKNOWLEDGMENT

We thank the DST (New Delhi) for financial assistance. Three of us are grateful (S. C., N. P., and R. K. S) to the CSIR (New Delhi) for Fellowships. We are also thankful to Prof. N. V. S. Rao of Assam University (Silchar) for POM micrograph of compound **6a**.

REFERENCES

[1] Reinitzer, F. (1888). *Monatsh. Chem.*, *9*, 421.
[2] Chandrasekhar, S., Sadashiva, B. K., & Suresh, K. A. (1997). *Pramana*, *9*, 471.
[3] Majumdar, K. C., Pal, N., Debnath, P., & Rao, N. V. S. (2007). *Tetrahedron Lett.*, *48*, 6330.
[4] Kumar, S. (2006). *Chem. Soc. Rev.*, *35*, 83.
[5] Tschierske, C. (1998). *J. Mater. Chem.*, *8*, 1485.
[6] Tschierske, C. (2001). *J. Mater. Chem.*, *11*, 2647.

[7] Tschierske, C. (2001). *Annu. Rep. Prog. Chem.*, *C 97*, 191.
[8] Tschierske, C. (2002). *Curr. Opin. Colloid. Interface. Sci.*, *7*, 69.
[9] Demus, D. (1989). *Liq. Crystal*, *5*, 75.
[10] Vorlander, D., & Apel, A. (1929). *Ber. Dtsch. Chem. Ges.*, *62*, 2831.
[11] Vorlander, D., & Apel, A. (1932). *Ber. Dtsch. Chem. Ges.*, *65*, 1101.
[12] Prasad, V. (2001). *Liq. Crystal*, *28*, 145.
[13] Niori, T., Sekine, F., Watanabe, J., Furukawa, T., & Takezoe, H. (1996). *J. Mater. Chem.*, *6*, 1231.
[14] Pelzl, G., Diele, S., & Weissflog, W. (1999). *Adv. Mater.*, *11*, 707.
[15] Prasad, V., Rao, S., & Krishna Prasad, D. S. (2000). *Liq. Crystal*, *27*, 585.
[16] Majumdar, K. C., Pal, N., & Rao, N. V. S. (2006). *Liq. Crystal*, *33*, 531.
[17] Majumdar, K. C., Mondol, S., Pal, N., & Sinha, R. K. (2009). *Tetrahedron Lett.*, *50*, 1992.
[18] Majumdar, K. C., Pal, N., Debnath, P., & Rao, N. V. S. (2007). *Tetrahedron Lett.*, *48*, 6330.
[19] Majumdar, K. C., Pal, N., Nath, S., Choudhury, S., & Rao, N. V. S. (2007). *Mol. Cryst. Liq. Cryst.*, *461*, 37.
[20] Majumdar, K. C., Chattopadhyay, B., Chakravorty, S., Pal, N., & Sinha, R. K. (2008). *Tetrahedron Lett.*, *49*, 7149.
[21] Majumdar, K. C., Chakravorty, S., Pal, N., & Rao, N. V. S. (2009). *Tetrahedron*, *65*, 152.
[22] Majumdar, K. C., Chakravorty, S., & Pal, N. (2009). *Mol. Cryst. Liq. Cryst.*, *503*, 112.
[23] De, P. (2004). *Synlett*, *10*, 1835.
[24] Matasuzaki, H., & Matasunga, Y. (1993). *Liq. Crystal*, *14*, 105.
[25] Sadashiva, B. K., Raghunathan, V. A., & Pratibha, R. (2000). *Ferroelectrics*, *243*, 249.
[26] Rouillon, J. C., Marcerou, J. P., Laguerre, M. H., Nguyen, T., & Achard, M. F. (1999). *J. Mater. Chem., 11*, 2946.
[27] Cambridge Soft Corporation: USA. (2006). Chem3D, version 10, Cambridge Soft.
[28] Frisch, M. J. (2004). GAUSSIAN 03 (Revision c.02); Gaussian, Wallingford CT.
[29] Eremin, A., Diele, S., Pelzl, G., Nadas, H., Weissflog, W., Salfetnikova, J., & Kresse, H. (2001). *Phys. Rev. E*, *64*, 051707.
[30] Yelamaggad, C. V., Hiremath Uma, S., & Shankar Rao, D. S. (2001). *Liq. Cryst., 28*, 351.
[31] Prajapati, A. K., Thakkar, V., & Bonde, N. (2003). *Mol. Cryst. Liq. Cryst.*, *393*, 41.
[32] Cseh, L., Csunderlik, C., & Costisor, O. (2005). *Chem. Bull.*, *50*, 64.
[33] Parra, M., Hernandez, S., Alderete, J., & Zuniga, C. (2000). *Liq. Cryst.*, *27*, 995.
[34] Yellamaggad, C. V., Shaskikala, I. S., Hiremath, U. S., Liao, G., Jakli, A., Rao, D. S. S., Prasad, S. K., & Li, Q. (2006). *Soft Matter*, *2*, 785.